THE SOFT X-RAY EXCESS IN EINSTEIN QUASAR SPECTRA.

Belinda J. Wilkes[2], Jean-Louis Masnou[1], Martin Elvis[2],
Jonathan McDowell[2] and Keith Arnaud[3]

[1]Observatoire de Paris-Meudon; [2] Harvard-Smithsonian Center for Astrophysics;
[3] NASA/Goddard Space Flight Center.

ABSTRACT.

We study the soft X-ray excess component for a signal-to-noise (S/N) limited sub-sample of 14 quasars taken from the WE87 (Ref. 1) sample observed with the *Einstein* IPC. Detailed analysis of the IPC data, combined with *Einstein* MPC data where possible, and use of accurate Galactic N_H values (Ref. 8) allows us to estimate the strength of any excess and to improve constraints on the spectral slope at higher X-ray energies. We find a significant excess in 9 of the 14 objects, confined in all but one case to below 0.6 keV and variable in the two cases where there are multiple observations. We investigate the relation of the soft excess to other continuum properties of the quasars.
Keywords: Quasars; Soft X-ray Excess; Full energy distributions; the blue bump.

1. INTRODUCTION.

Recent soft X-ray observations have shown that active galactic nuclei (AGN) and quasars commonly show strong soft excess emission above the extrapolation of their higher energy slopes (Ref. 1 (WE87), 2,3 (TP89),4). A summary is given in Ref. 5. These excesses occur primarily in the C-band, (*i.e.* below the <0.28 keV Carbon edge) and seem to rise steeply to lower energies, although information is generally limited to a single flux point due to the lack of energy resolution at these low energies. A simple extrapolation of the optical/UV "blue bump" component of the continuum predicts a much stronger X-ray flux than is observed in quasars; thus the X-ray spectrum must turn up at low energies to meet the UV. It is tempting to identify this new, soft excess component in the X-ray spectra of quasars as such a turn-up.

The blue bump is generally modeled as thermal emission from an accretion disk possessing a range of temperatures (Ref. 6,7), an interpretation which is enticing both observationally and theoretically. An obvious identification of the soft X-ray excess is the high-energy tail of the thermal emission (Ref. 14,15). In this case it would originate in the hottest, innermost edge of the accretion disk at $\sim$ 10 Schwarzschild radii. Should this be confirmed, the excess will provide far stronger constraints on the physical conditions of this part of the disk than have been possible so far. Quantitative measurement of the soft excess is thus of the utmost importance.

As stated above, measurements to date have been confined to a single discrepant flux point at low energies providing very limited spectral information except in a handful of cases. In this paper we use the highest S/N IPC observations of quasars from the WE87 sample, combined with the higher energy (2-10 keV) Monitor Proportional Counter (MPC) data where it is available and accurate Galactic N_H values (Ref. 8). This improved data makes a two-component fit useful, allows us to determine the strength of the soft excess and to better determine the slope and normalization of the high energy fit. We then search for relations between the excess strength and other continuum properties of these objects in particular the strength and shape of the blue bump.

2. ANALYSIS.

2.1 The Data.

The sample of quasars studied by WE87 included all those available in the IPC data bank which were observed on-axis with sufficiently high S/N to allow useful constraints to be placed on the spectral slope. Of these 33 quasars, half were radio- and half optically-selected. For the current study we have selected from the sample those observations with $\gtrsim$1200 net counts in the IPC. This yields a subset of 14 quasars, 5 of which are radio-loud. A list of these objects and the X-ray observations (IPC and MPC) used is given in Table 1. The redshift and the Galactic column density of neutral hydrogen (Ref. 8) are also given. PG1211+143 is included in this table for completeness although it is not re-analyzed here (Sect. 2.3).

The IPC X-ray data were analyzed following the standard procedure described in Ref. 1,9. Briefly, counts were obtained from a 3' circle centered on the position of the source. A correction was applied for counts falling outside this circle and background counts were estimated from a 5'-6' annulus, also centered upon the source position. The energy range of

Proc. 23rd ESLAB Symp. on Two-Topics in X-Ray Astronomy, Bologna, Italy, 13-20 September, 1989 (ESA SP-296, Nov. 1989).

the IPC was 0.15-3.5 keV. The first bin of the pulse height distribution was excluded since the errors due to the lower level discriminator are not well determined.

In this new analysis we have also used data from the Monitor Proportional Counter (MPC) for which > 500 counts were detected. Apart from a couple of early studies (Ref. 9, 10) the MPC has been little used for quasars until now due to systematic uncertainties in the background subtraction process for these faint sources. These uncertainties have now been reduced and quantified for all observations prior to Oct 1980 (Ref. 11) allowing simultaneous fitting of IPC and MPC data. The MPC data have the advantage of covering a higher energy range, allowing a better determination of the high energy component. The MPC counts are distributed into 8 pulse height channels, from 1.2 to 20 keV, although channels 7,8 (> 10 keV) were not used in this analysis as they provide no additional constraint on the spectral fits. Thus the total energy range of our study is generally 0.1-10 keV.

2.2 Spectral Analysis.

A single power law model was fitted to the combination of IPC and MPC data assuming that there is negligible absorption intrinsic to the quasar (WE87) and using accurate, small beam (21') values for Galactic column densities (N_H, Ref. 8). The errors in these measured N_H values are estimated to be < 6%, negligible for our purposes. The N_H value for 3C273 is taken from Ref. 12, again with a negligible error. The slope and normalization of the power law were determined with N_H fixed at the Galactic value.

The single power law gives a poor fit ($P(\chi^2) < 10\%$) for 10 of the 16 observations analyzed here. In most cases the residuals show that the low energy channels are significantly above the fit providing evidence that a soft excess is present. In order to quantify this possible component a broken power law model was then fitted to the data. This model was chosen as the simplest way to estimate the strength of the soft excess, which is all we can do with our low resolution data. The spectral shape of the component cannot be determined.

Table 1: Observational Details.

Name	Redshift N_H^a	I/MPC	Seq.No.	Date	Net Counts	T_{exp}(sec)
0026+129	0.142	IPC	5417[b]	01:04:81	2678±55	11152
PG	4.93	MPC	518	01:07:79	1413	2744
0054+145	0.171	IPC	5418	07:19:80	1289±39	11735
PHL 909	4.20	IPC	4248	07:02:79	424±23	3717
0205−024	0.155	IPC	3978	07:20:79	1237±38	7608
NAB	2.99					
0637−752	0.656	IPC	8494	12:14:80	1199±39	7480
PKS	5.00[c]	MPC	5404	10:30:79	661	860
1028+313	0.177	IPC	4256	05:24:79	1167±37	6595
B2	1.98	MPC	4256		724	3768
1219+756	0.07	IPC	5424	04:20:80	6437±85	13113
MKN 205	2.74	MPC	5424		8667	11100
1226+023	0.158	IPC	2037	06:20:79	4534±68	1740
3C273	1.80[d]	MPC	2037		3910	696
"		IPC	5692	01:01:80	9362	3911
		MPC	5692		17437	3523
"		IPC	9310	12:13:80	6687	1668
1253−055	0.538	IPC	4645	07:14:80	3279±65	25095
3C279	2.22	MPC	4645	07:14:80	2128	14541
1426+015	0.086	IPC	5348[e]	08:03:80	1231	2034
PG	2.64	MPC	5348		1734	1843
"		IPC	10374[f]	01:05:81	4748±91	13210
1501+106	0.036	IPC	6713	01:18:80	1663±42	1475
MKN 841	2.23	MPC	6713		1023	983
1613+658	0.129	IPC	10375[g]	02:06:81	2217±51	7209
PG	2.66					
2130+099	0.061	IPC	1971	05:03:80	862±33	4987
II Zw 136	4.20	IPC	1972	04:20:81	485±23	1429
2135−148	0.20	IPC	5426	05:10:80	2521±54	12902
PHL 1657	4.45	MPC	5426		1914	8560

a: Galactic equivalent hydrogen column density in atoms cm^{-2} from Ref. 8 (unless otherwise noted).
b: Sum of sequence numbers 5417,9550,9551,9552,9553
c: Ref. 28
d: Ref. 12
e: Spectral results reported in Ref. 9.
f: sum of sequence numbers: 10374,10390,10391,10392,10393
g: sum of sequence numbers: 10375,10394,10395,10396,10397

Table 2: Parameters for the Broken Power Law Fits:
a: Observations with a Soft Excess.

Name	Seq. No.	Bins χ^2	α_{HE} α_{LE}	f(1 keV)[a]	f(0.2 keV)[b]	$f_{OXS}(0.2)$[c]	Radio L/Q
0054+145	I5418	21	0.41	$0.52^{+0.04}_{-0.04}$	$1.02^{+0.33}_{-0.26}$	$4.16^{+1.63}_{-1.58}$	RQ
	I4248	11.5	1.9				
0205+024	I3978	11	1.2	$0.58^{+0.06}_{-0.06}$	$4.0^{+2.4}_{-1.5}$	$14.8^{+4.4}_{-5.0}$	RQ
		8.4	2.6				
1028+313	I4256	12	0.74	$0.80^{+0.07}_{-0.07}$	$3.65^{+0.70}_{-0.70}$	$4.2^{+2.6}_{-2.6}$	RL
	M4256	5.1	1.6				
1219+756	I5424	16	0.85	$2.29^{+0.08}_{-0.08}$	$9.1^{+1.2}_{-1.0}$	$7.0^{+2.1}_{-2.9}$	RL
	M5424	13.3	1.4				
1226+023	I5692	16	0.54	$10.0^{+0.2}_{-0.2}$	$23.9^{+1.4}_{-1.3}$	$22.5^{+3.4}_{-3.6}$	RL
	M5692	30.3	1.1				
	I9310	8	0.49	$18.9^{+0.7}_{-0.7}$	$41.5^{+6.1}_{-5.4}$	$31.3^{+13.3}_{-13.8}$	RL
		5.6	1.0				
1426+015	I10374	8	0.94	$1.73^{+0.09}_{-0.09}$	$7.82^{+2.0}_{-1.6}$	$9.3^{+4.0}_{-4.4}$	RQ
		7.2	1.7				
1501+106	I6713	16	1.02	$4.2^{+0.3}_{-0.3}$	$21.8^{+5.7}_{-4.5}$	$25.8^{+8.8}_{-9.9}$	RQ
	M6713	7.8	1.7				
2130+099	I1971	10	0.81	$0.91^{+0.08}_{-0.07}$	$3.40^{+1.50}_{-2.13}$	$19.4^{+5.4}_{-5.3}$	RQ
	I1972	3.2	2.6				

b: Observations without a Soft Excess.

0026+129	I5417	14	0.91	$1.39^{+0.07}_{-0.07}$	$6.1^{+1.4}_{-1.1}$	$-0.8^{+4.5}_{-4.1}$	RQ
	M518	10.2	0.8				
0637−752[d]	I8494	15	0.46	$0.95^{+0.03}_{-0.03}$	−2.0	−2.6	RL
	M5404	6.3					
1226+023	I2037	15	0.58	$12.1^{+0.3}_{-0.4}$	$30.7^{+1.9}_{-3.5}$	$7.5^{+7.5}_{-5.7}$	RL
	M2037	26.2	0.8				
1253−055	I4645	16	0.74	$0.66^{+0.03}_{-0.03}$	$2.2^{+0.4}_{-0.3}$	$-0.9^{+0.6}_{-0.6}$	RL
	M4645	31.0	0.3				
1426+015	I5348	15	1.18	$3.0^{+0.2}_{-0.2}$	$19.8^{+6.3}_{-4.7}$	$2.5^{+9.2}_{-10.3}$	RQ
	M5348	14.7	1.3				
1613+658	I10375	11	1.10	$1.3^{+0.07}_{-0.07}$	$7.9^{+2.4}_{-1.8}$	$3.0^{+3.1}_{-2.4}$	RQ
		6.3	1.4				
2135-148	I5426	16	0.76	$1.13^{+0.07}_{-0.07}$	$3.8^{+0.7}_{-0.6}$	$-0.4^{+1.9}_{-1.9}$	RL
	M5426	27.6	0.7				

a: Normalization in μJy
b: Flux of high energy component at 0.2 keV in observed frame, corrected for Galactic absorption in μJy
c: Flux in Excess at 0.2 keV (observed frame), corrected for Galactic absorption in μJy
d: The errors on fit parameters could not be estimated, however there is clearly no excess present.

N_H was again fixed at the Galactic value and the break energy between the two components set at 0.6 keV. The break energy must be in the octave $\sim 0.3 - 0.6$ keV for a soft excess to be detected in these data. In practice the exact value used for the break energy had little effect on the estimated flux in the soft excess (see below).

Instead of the conventional fit to power-law indices, the fit was parameterized in terms of the normalization (f(1 keV)), the flux at 0.2 keV of the extrapolated high energy component (f_{HE}(0.2keV)) and the flux at 0.2 keV in the excess (f_{XS}(0.2keV)). All three parameters were allowed to vary freely. This procedure yields tighter constraints on the fitted parameters and a direct determination of the strength of the excess. A small change in flux leads to a large change in slope for slopes as steep as those of the soft excess. The fitted slope also depends strongly on the assumed break energy whereas the 0.2 keV flux does not. A change of break energy from 0.6 keV to 0.4 keV led to a mean increase in the f_{xs}(0.2keV) flux of 0.8σ. While this is not a significant increase, it does indicate that our use of 0.6 keV leads to a conservative estimate of the f_{xs}(0.2keV) flux. The results for normalization, both fluxes, 1σ errors and the χ^2 values are given in Table 2. The fluxes are corrected for Galactic absorption. The errors on these fluxes are the 1σ errors for each interesting parameter: f_{HE}(0.2keV), f_{XS}(0.2keV) and f(1 keV), *ie.* using a $\Delta\chi^2 = 1.0$ (Ref. 18). The low and high energy slopes derived from these fits are also given in Table 2 for illustration and comparison. Since they are not fitted parameters, no formal error bars are quoted although they are implied by the errors on the fluxes.

Additional fits were made using a black-body spectrum for the soft excess in order to estimate the temperatures required and also with modified abundances to determine the effect of ionized hydrogen along the line-of-sight through our Galaxy.

2.3 Notes on Individual Objects.

0637-752 has no accurate Galactic N_H measurement due to

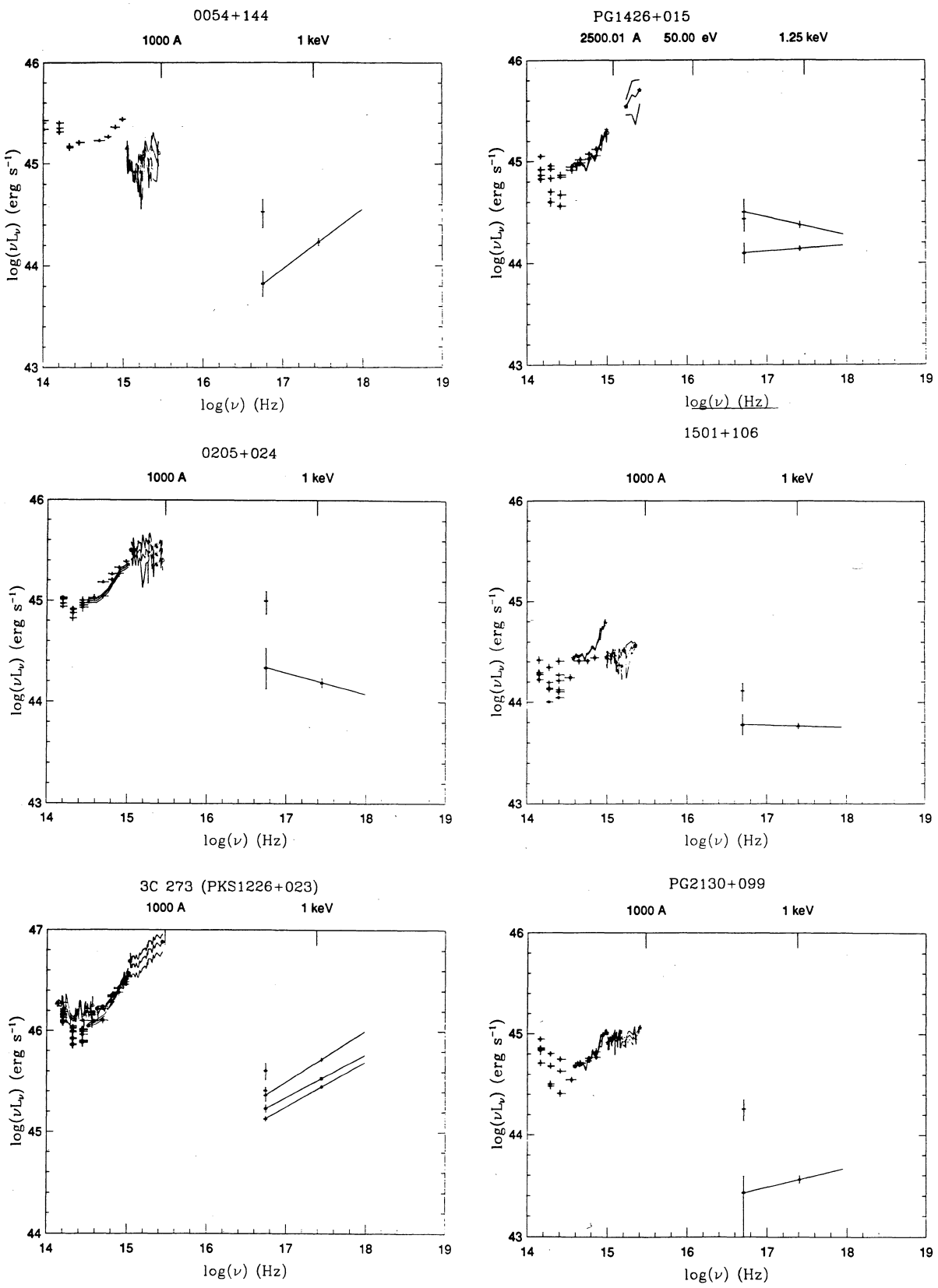

Figure 1. 100μ - 10 keV energy distributions for those quasars with detected soft excess components. The excess is shown as a 0.2 keV flux point above the high energy power law.

its negative declination. The error on its value (Ref. 28) is estimated at $\pm 1.0 \times 10^{20} cm^{-2}$ (Ref. 9). Fits were performed with the $\pm 1\sigma$ values for N_H and no evidence for a soft excess was found in either case.

PG1211+143 is already known to have a strong soft excess (Ref. 13-15). This soft excess is unusual since it displays a break around 2 keV, a much higher energy than the 0.3-0.6 keV generally seen. The MPC data for this object is unreliable, as are all observations made after October 1980, due to the lack of a reliable background subtraction algorithm. (N.B. This was not known at the time of the earlier study (Ref. 14)). The lack of higher energy data combined with the high break energy between the excess and the high energy components conspires to make it difficult to determine the parameters of this spectrum so it is not included in our analysis.

PHL 1657 (2135-148) has a peculiar spectrum which is not fitted well by either a power law or a black body form. It seems to be gradually steepening to higher energies causing a broken power law fit to show a marginally significant deficit at soft energies. This kind of spectrum is more characteristic of BlLac objects, where a steepening is seen around 2-3 keV, than quasars (Ref. 16,17)

3. RESULTS.

3.1 The Soft Excess.

Based on the results of the fits described above, a soft excess above a single power law fit was found, at the 90% confidence level, in 8 of the 13 quasars analyzed here and in a total of 9 observations (Table 2). TP89 (Ref. 3) report that 50% of their unabsorbed, radio-quiet, Seyfert 1 galaxies in their EXOSAT sample possess a significant soft excess. These results imply that soft excess components are common in both quasars and Seyfert 1 galaxies over a wide range in luminosity. The 100μ to 10 keV energy distributions for six of the objects having an excess are shown in Figure 1.

It should be noted that the f_{XS}(0.2keV) fluxes reported here are likely to be underestimates for a number of reasons in addition to our choice of break energy discussed earlier. The presence of an intrinsic absorbing column in a quasar, which was assumed here to be absent, would cause us to underestimate the soft X-ray flux, as would the presence of ionized hydrogen along the line-of-sight (see below). Also, since the excess is only just visible at the low end of our energy range, a small redshift would make it undetectable.

3.1.1 Relation to Redshift. No significant dependence on redshift was found but the two objects with the highest redshift (z>0.5): 0637-752; 1253-055; have no excess. A redshift of 1.0 would generally shift the excess below our observed energy range. The magnitude and errors of our detected fluxes at 0.2 keV suggest that a redshift of 0.5 would be sufficient to make it undetectable in most cases.

3.1.2 Relation to Radio Properties. The current sample includes 5 radio-loud objects and 9 radio-quiet. 2 of the 5 radio-loud objects and 7 of the 9 radio-quiet show excesses. The probability of seeing such a distribution if the parent populations of these two samples are the same is 18% (Fischer test), *i.e.* there is no evidence that radio-loud and radio-quiet objects are different in their excess properties. Not surprisingly therefore we found no significant correlation between radio-loudness (as defined by WE87) and soft excess strength.

Two of the three radio-loud quasars with no soft excess have high redshift implying that the excess is redshifted out of the IPC energy range: The third is a lobe dominated radio source (R=1.1, Ref. 19) while both those with an excess are core dominated (R=0.2,0.8 for 1028+313 and 3C273 respectively). Lobe-dominated radio sources are thought to be edge-on systems while core-dominated are face-on (Ref. 20). If the soft excess is part of the blue bump, which is generally believed to be emitted by an accretion disk, we would expect to see it only in relatively face-on systems. Although our sample is far too small to test this hypothesis, we note that the results so far are consistent with this picture.

3.1.3 Variability. The X-ray flux is variable in both objects for which more than one epoch of high S/N data was available: 3C273, 1426+015.

There are three observations of 3C273 over 17 months. The first observation shows a marginal excess the 90% confidence range on the excess flux encompasses zero. In the following two observations the excess is highly significant (Table 2).

The 1 keV flux is also variable with a decrease of 20% over 6 months followed by an increase of 70% over 11 months. This implies that for 3C273 both soft excess and high-energy components are variable and the variations are not correlated. A similar result has been found in recent ***Ginga*** observations of 3C273 (Ref. 21).

There are two observations of 1426+015, 5 months apart. The first shows no excess while the second shows a significant excess and a 40% decrease in 1 keV flux. The apparent variation in slope (Fig. 1.) is not significant. This kind of variation is consistent with a constant excess which is not visible when the high energy flux is high.

3.1.4 The 'Canonical' Power Law. First results on the spectra of AGN, mostly Seyfert 1 galaxies, showed a surprising uniformity of the 2-10 keV power law slope: 0.65±0.15 (Ref. 22). This led to much discussion of a 'canonical' X-ray power law for AGN. More recent results have shown a larger range in the power law slopes both at lower energies (0.2-3.5 keV, WE87, Ref. 22-24) as well as in the 2-10 keV energy band (TP89, Ref. 25). Since the current sample covers both energy ranges it is of interest to see how it compares.

Although the mean energy index for our sample is 0.76±0.29, where the dispersion indicates the spread in observed values, we find that only 3 of the 10 objects which have MPC data (*i.e.* our fits cover 0.6-10 keV) are consistent with a 0.7 energy index at the 99% level. This is less than half the

sample and supports earlier results that show a real range is present. Of those with only IPC data (*i.e.* <3.5 keV), 3 of the 4 are consistent with 0.7 at the 99% level. These results confirm that, while 0.7 remains the average slope for quasars and Seyfert 1 galaxies, there is no unique 0.7 power law slope which applies to them all.

Notably the 3 objects consistent with a 0.7 slope are all radio-loud: 0637-752, 1028+313, 1253-055. A comparison with the IPC results of WE87 shows that these three, along with 3C273 (Seq. No. 2037) have a steeper slope when the MPC is included, while the radio-quiet objects show no change. This is apparent in Fig. 2 where the comparison is plotted for those objects with MPC data. This suggests that radio-loud quasars have slightly steeper slopes in the MPC energy range than in the IPC while radio-quiet quasars have the same slope (Fig. 2). This is in contrast to the flattening of the radio-quiet quasars at higher energies predicted by WE87. There are too few objects to draw firm conclusions but these results suggest that the radio-loud linked component of WE87 steepens in the 2-10 keV range to a more 'canonical' slope of ~ 0.7. Another possibility, which is currently under investigation, is that the two instruments are not correctly normalized relative to one another in our analysis. If confirmed the steepening would partially explain the apparent discrepancy between the low and high energy slopes, although the steepness of the radio-quiet quasars when compared with the lower luminosity Seyfert1 galaxies remains unexplained.

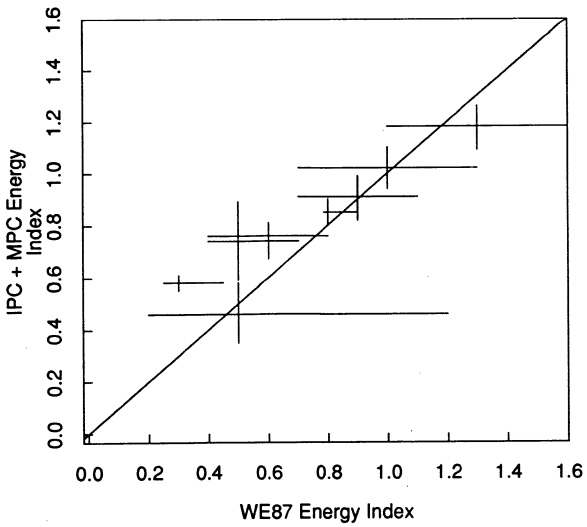

Figure 2. Comparison of the slopes determined in this study for those objects with MPC data with the IPC results of WE87.

3.1.5 Black Body Fits to the Soft Excess. We have no good spectral information for the soft excess component which compelled us to assume a specific form (in this case a power law) as a convenient way to parameterize the data. Since the excess is thought to be the high energy tail of a thermal component from the inner regions of an accretion disk, a black body form would naively seem more physical. However, model calculations have demonstrated that other effects, such as comptonization (Ref. 15), are likely to modify the spectrum from these regions. For comprison with other studies we performed a two-component fit with a simple black body form as the low energy component. We found that the excess values determined were consistent with those using the broken power law model but the error bars were much larger presumably due to the steepness of the spectral form. We were, however, able to estimate an upper limit for the temperature of a simple thermal competent. In Table 3 we list upper limits (T_{max} = kT $+1\sigma$, $\delta\chi^2$=1.0) upper limits to the temperature for those objects which have a soft excess component.

3.1.6 The effect of Ionized Gas above the Galactic Disk. Recent searches for the presence of ionized gas above the disk in our Galaxy have led to estimates that $\sim$ 37% of the hydrogen along a line-of-sight through the Galaxy is ionized (Ref. 26). In this case the total Galactic X-ray column, computed assuming the observed neutral hydrogen column density accounts for all the hydrogen, will be underestimated. This would result in our underestimating the strength of the soft excesses deduced for the quasar spectra. We checked the magnitude of this effect for our sample by increasing the metal contribution to the X-ray column by 37% and repeating our broken power-law fits. We found that the number of detected excesses increased by 3 to 12 of the 14 quasars and the 0.2 keV excess fluxes doubled.

Since the ionized hydrogen result (Ref. 25) is preliminary, covering only two lines-of-sight at this stage, we take this study no further here. However the presence of ionized gas would clearly have important implications for the modeling of soft X-ray spectra for any extragalactic source. Indeed variations of the soft X-ray source density in the ROSAT all-sky survey may be an excellent means of mapping this component of the interstellar medium.

3.2 Relation of soft excess to other properties.

The soft excess flux was checked for dependence on the high energy slope as a consistency check on our procedure. No dependence was found, confirming that the high energy fit component is not significantly affected by the presence of a soft excess if a two-component model is used. Other diagnostic checks included a search for correlations of the soft excess with IPC net counts or the Galactic N_H. No dependence on either of these parameters was found. Two of the five objects with high N_H ($> 4.0 \times 10^{20} cm^{-2}$) have a significant soft excess and one of the three remaining has a relatively high redshift.

A search for a relation between the soft excess and the strength of the blue bump proved negative. The discovery of such a direct relation would provide strong confirmation of the identification of the excess as the high energy tail of the blue bump component. However, a negative result does not rule out this possibility. As mentioned above there are many effects which could change the observed soft excess strength or mask its existence completely so a simple relation is not required (Sect. 3.1). In addition the presence of a patchy absorber in the quasar itself results in an apparently very similar soft excess due to leakage of the high energy component (Ref. 3, Sect. 4.).

Table 3: Parameters for the Black Body and Power Law Fits:

Name	IPC MPC	T_{max}(keV)
0054+145	I5418	0.13
	I4248	
0205−024	I3578	0.04
1219+756	I5424	0.04
	M5424	
1226+023	I2037	0.10
	M2037	
	I5692	0.11
	M5692	
	I9310	0.04
1426+015	I10374	0.05
1501+106	I6713	0.10
	M6713	
2130+099	I1971	0.09
	I1972	

3.3 The Radio-loudness/α_E Correlation.

WE87 reported a correlation between the radio-loudness and X-ray slope (equivalent to the high energy slope here) of the quasars in their sample in the sense that the more radio-loud the object, the flatter the X-ray slope. The possibility that this correlation was caused by the presence of an unresolved soft excess (<0.3 keV), similar to those found by EXOSAT was raised by TP89. This explanation was considered unlikely by WE87 after a study of the IPC data with E>0.6 keV failed to show the flattening of the X-ray slopes expected in this case. In addition this interpretation would require that the soft excess be stronger in radio-quiet than in radio-loud quasars, an effect which was neither apparent in the WE87 nor in the current data (Sect. 3.1.2). WE87 interpreted the correlation as due to a changing mix of two components, one of which is linked with the radio emission and neither of which is the soft excess.

The extension of the WE87 spectra to higher energies in this paper allows a better test of this question. Fig. 3 shows the high-energy slope versus radio-loudness for this sub-sample superposed on WE87's origin figure. The correlation is clearly present and is significant at the 0.5% level. This result, combined with the lack of a relation between the soft excess strength and radio-loudness of a quasar described above, strengthens the WE87 hypothesis that the soft excess does not cause the radio-loudness/α_E correlation.

Kruper, Urry and Canizares (Ref. 27, KUC89 hereafter) also find a radio-loudness/α_E correlation in their study of IPC Seyfert 1 galaxies. although only 6 of their well-constrained sample are radio-loud. No correlation between X-ray slope and radio-loudness was found in the sample of Seyfert 1 galaxies studied by EXOSAT at higher energies (2-10 keV, TP89). However this sample contains only 2 radio-loud objects. TP89 note that, for those objects where the soft excess is resolved, there is a tendency for the few higher luminosity objects, which tend to be more radio-loud (Ref. 29), to have flatter high-energy X-ray slopes.

KUC89 also report that individual Seyfert 1s observed with both HEAO1-A2 and the IPC have steeper IPC slopes, suggesting that a flatter component contributes to the higher energy region of A2, as predicted in the WE87 picture. However the radio-quiet quasars observed here do not confirm this flattening to higher energies.

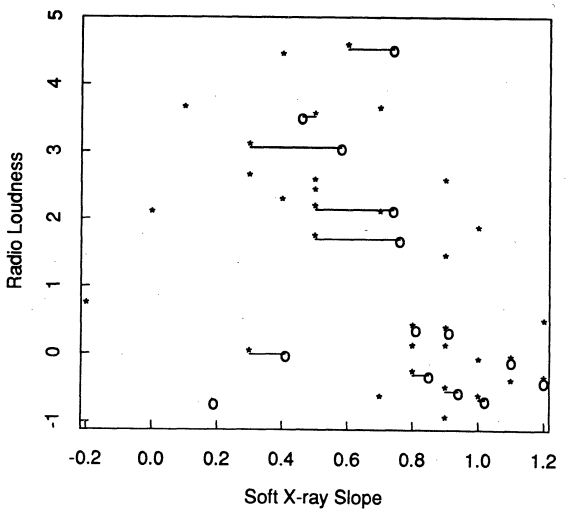

Figure 3. Radio Loudness, X-ray Slope correlation for the current analysis (o) compared with the original plot of WE87 (*). Points which correspond to the same objects are indicated.

4. DISCUSSION.

4.1 The Soft Excess.

It is now very clear that soft X-ray excess components are a common continuum feature of all kinds of AGN including Seyfert 1s, radio-loud and radio-quiet quasars. Analysis of EXOSAT data has revealed two main types of excesses (Ref. 3, 30): those due to a distinct soft emission component and those due to leakage of the higher energy component through a patchy absorber. The current analysis cannot, due to the low resolution of the data, distinguish between these two possibilities. It is likely that examples of both are present. This of course, along with all the other possible ways in which the soft excess can be changed between its emission and our observation (Sect. 3.1), conspires to make it difficult to draw any definite conclusions about its identity. The high energy tail to the blue bump remains the most attractive candidate and the presence of both components, regardless of the class of AGN, might be considered as circumstantial support for this picture. But we cannot rule out such alternatives as the possibility that the soft excess is a completely new component or that there is no distinct component and the high energy component steepens below $\sim$ 0.3 keV (Ref. 31, 32). More, higher resolution, observations are clearly necessary. ROSAT will provide the next opportunity for observations. The definitive test of the blue bump identification would be simultaneous UV and soft X-ray monitoring.

4.2 The High Energy Component.

The slope of the high energy (0.6-10 keV) component is confirmed to be related to the radio-loudness of a quasar, as suggested in WE87 (Ref. 1). The presence of an additional, radio-linked, X-ray component, possibly due to synchrotron self-Compton emission, was first suggested to explain the significantly stronger X-ray flux from radio-loud quasars (Ref. 29). Given this model, the observed difference in slope between radio-loud and -quiet quasars is not a surprise but simply confirmation of differing emission mechanisms in the two classes of object.

5. REFERENCES.

1. Wilkes, B. J. and Elvis, M. 1987 (WE87) Ap.J. **323**, 243

2. Arnaud, K. A., Branduardi-Raymont, G., Culhane, J. L.,Fabian, A. C., Hazard, C.,McGlynn, T. A., Shafer, R. A., Tennant, A. F. and Ward, M. J. 1985 M.N.R.A.S. **217**, 105

3. Turner, T. J. and Pounds, K. A. 1989 (TP89) M.N.R.A.S. *in press*

4. Branduardi-Raymont, G., Mason, K. O., Murdin, P. G. and Martin, C. 1985 M.N.R.A.S. **216**, 1043

5. Elvis, M., Wilkes, B. J. and McDowell, J. C. 1989 in Extreme Ultraviolet Astronomy, Pergammon, New York, *in press*

6. Shields, G. A. 1978 Nature **272**, 706

7. Malkan, M. A. and Sargent, W. L. W. 1982 Ap.J. **254**, 22

8. Elvis, M., Lockman, F. J. and Wilkes, B. J. 1989 *A.J.* **97**, 777

9. Elvis, M., Green, R. F., Bechtold, J., Schmidt, M., Neugebauer, G., Soifer, B. T., Matthews, K. and Fabbiano, G. 1986 Ap.J. **310**, 291

10. Halpern, J. 1981 PhD. Thesis, Harvard University.

11. Arnaud, K. A. 1989, *in preparation*

12. Dickey, *et al.* 1978 Ap.J.Suppl **36**, 77

13. Elvis, M., Wilkes, B. J. and Tananbaum, H. 1985 Ap.J. **292**, 357

14. Bechtold, J., Czerny, B., Elvis, M., Fabbiano, G. and Green, R. F. 1986 Ap.J. **314**, 699

15. Czerny, B. and Elvis, M. 1987 Ap.J. **321**, 305

16. Madejski, G. M and Schwartz, D. A. 1989 in BL Lac Objects 10 Years After., Springer-Verlag, 267

17. Barr, P., Giommi, P., Tagliaferri, G., Maccagni, D. and Garilli, B. 1989 in BL Lac Objects 10 Years After. Springer-Verlag, 290

18. Avni, Y. 1976 Ap.J. **210**, 642

19. Browne, I. W. A. and Murphy, D. W. 1987 M.N.R.A.S. **226**,601

20. Orr, M. J. L. and Browne, I. W. A. 1982 M.N.R.A.S. **200**,1067

21. Turner, M. J. L. *et al.* 1989 M.N.R.A.S. *submitted*

22. Mushotzky, R. F. 1984 *Adv. Sp. Res.* **3**,157

23. Worrall, D. M. and Wilkes, B. J. 1989 Ap.J. *submitted*

24. Brunner, H., Worrall, D. M., Wilkes, B. J. and Elvis, M., *this volume.*

25. Turner, M. J. L., *this volume*

26. Reynolds, R. J. 1989 Ap.J. **339**, L29

27. Kruper, J. S., Urry, C. M. and Canizares, C. R. 1989 (KUC89) Ap.J. *submitted*

28. Heiles, C. and Cleary, M. N. 1979 Aust. J. Phys. Suppl. **47,1**

29. Zamorani, G. *et al.* 1981 Ap.J. **245**, 357

30. Pounds, K. A., *this volume*

31. Schwartz, D. A., Qian, Y. and Tucker, W., *this volume*

32. Band, D. L. and Grindlay, J. E. 1986 Ap.J. **308**, 576